

Multiplicity and Transverse Sphericity dependence of $\langle p_T \rangle$ fluctuations of charged particles in p–p collisions at $\sqrt{s} = 7$ and 13 TeV

Subhadeep Roy,^{1,*} Tulika Tripathy,^{1,†} and Sadhana Dash^{1,‡}

¹*Indian Institute of Technology Bombay, Mumbai 400076, India*

The multiplicity dependence of event-by-event fluctuations in mean transverse momentum, $\langle p_T \rangle$, of charged particles has been studied in p–p collisions at $\sqrt{s} = 7$ TeV and 13 TeV using the PYTHIA 8 event generator. The charged particles were selected in kinematic range of $0.15 < p_T < 2$ GeV/ c and $|\eta| < 0.8$. The dynamical fluctuations would indicate towards the correlated emission of particles. The measurements in A–A and p–p collisions has shown a decrease in the strength of $\langle p_T \rangle$ fluctuations with the average charged particle multiplicity. The effects of various microscopic processes like color reconnection and multi-partonic interactions has been studied. A minimal dependency on the collision energy is also observed. Furthermore, the fluctuation observables are investigated in the intervals of transverse sphericity in order to comprehend the relative contributions resulting from hard scattering and underlying events. The present study would act as a baseline for future measurements in A–A as well as p–p collisions at the LHC.

I. INTRODUCTION

The search for event-by-event fluctuations in dynamical quantities, such as mean transverse momentum ($\langle p_T \rangle$) in heavy-ion collisions is primarily motivated by the search for the presence and characterization of the phase transition between a quark-gluon plasma (QGP) and hadron gas state [1–3]. One can quantify this search by looking for excess fluctuations of thermodynamic quantities like temperature. The event-wise $\langle p_T \rangle$ can be taken as a proxy for local temperature and hence the study of its event-by-event fluctuation has a thermodynamic context. The temperature fluctuations are related to the heat capacity of the system. The non-monotonic behaviour of heat capacity characterizes a phase transition and hence the study of event-by-event $\langle p_T \rangle$ fluctuations could reveal important information about the formation of QGP [4].

The recent measurements by the STAR [1, 5] and ALICE [2] experiment at RHIC and LHC reported that the strength of dynamical $\langle p_T \rangle$ fluctuations decreased with event multiplicity (or cen-

trality) in heavy-ion collisions. The observation was attributed to the onset of thermalization, collectivity, jet suppression, presence of di-jets and minijets and other processes. The interesting studies showing the $\langle p_T \rangle$ fluctuations and their correlations with radial flow and elliptic flow in heavy-ion collisions can be found in the references [6, 7]. It remains questionable whether the system created in small systems like p–p or p–A collisions exhibit collectivity as observed in A–A collisions. This can be addressed by studying particle production mechanisms, their correlations etc. as a function of the event shape and particle multiplicity. Recent experimental results of $\langle p_T \rangle$ in p–p collisions [2] suggest that, high-multiplicity events are mostly produced by multiple parton interactions (MPIs) [8]. The data exhibited a power-law trend with charged particle multiplicity density, as expected from the independent superposition scenario of independent multi-partonic interactions. However, the slight deviation of the power-law index from 0.5 indicated towards non-trivial fluctuations. In PYTHIA 8 [9], the observed strong correlation between the particle multiplicity and $\langle p_T \rangle$ has been attributed to the mechanism of color reconnections (CR) between hadronizing strings [11–13]. The color strings can also overlap with each other to form color ropes that act coherently in high-multiplicity events [14, 15]. This

* subhadeep.roy@cern.ch

† tulika.tripathy@cern.ch

‡ sadhana@phy.iitb.ac.in

overlap region causes a pressure gradient, thereby shoving the strings in the outward direction creating similar effects as observed in hydrodynamic scenario. The color reconnections together with the rope hadronization could explain some of the high-multiplicity observables in p–p collisions [16–18]. A similar mechanism of collective relativistic string hadronization is also implemented in the EPOS model which describes a wealth of LHC data in p–p, p–Pb, and Pb–Pb collisions [19].

In this work, an attempt has been made to study the $\langle p_T \rangle$ fluctuations in p–p collisions at collision energies, $\sqrt{s} = 7$ TeV and 13 TeV as a function of multiplicity and different transverse sphericity classes using PYTHIA 8 generator. The fluctuation is generally quantified by the second moment of the distribution and the two-particle correlator has been used to study the interplay of various processes. The higher moments, namely the third and fourth moment were also studied as a function of multiplicity to shed additional lights on higher order correlations in multi-particle production mechanism. The additional effects of color reconnection as well as the formation of ropes were also studied. This study would act as a baseline for future measurement in A–A and p–p systems.

II. TRANSVERSE SPHEROCITY

The study of various observables in terms of event shape variables such as transverse sphericity, thrust etc. helps to disentangle the contributions from hard and soft (scattering) processes of particle production. The transverse sphericity is a tool which characterises the event into jet-like or isotropic events [20–22]. It is defined for a unit transverse vector, $\hat{n}(n_T, 0)$, which minimizes the ratio

$$S_0 = \frac{\pi^2}{4} \min_{\hat{n}} \left(\frac{\sum_i |\vec{p}_{T_i} \times \hat{n}|}{\sum_i p_{T_i}} \right)^2 \quad (1)$$

This unit vector coincides with the transverse direction of the momentum, \vec{p}_T which makes the S_0 infrared and collinear safe. The sum runs over

all the particles considered in the kinematic acceptance. Events with $S_0 \rightarrow 0$ are likely to be dominated by a single hard scattering, producing a jet-like structure (**Jetty**). In contrary, $S_0 \rightarrow 1$ implies that particles are produced through several softer interactions, giving an **isotropic** distribution. An illustration of the two limits in the azimuthal plane is presented in Figure 1. To replicate

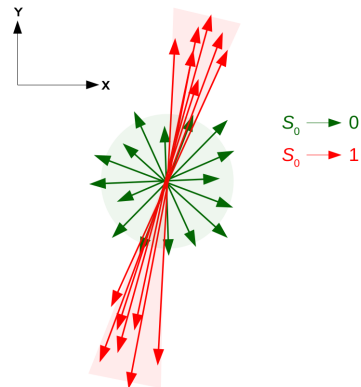


FIG. 1: Illustration of the typical topologies for the two S_0 limits in the azimuthal plane.

the same circumstances as the ALICE experiment at the LHC, the transverse sphericity distributions are chosen in the pseudo-rapidity range of $|\eta| < 0.8$ with a minimum constraint of 5 charged particles with $p_T > 0.15$ GeV/c. The various percentiles of the whole S_0 distribution are used for the selection of Jetty (0-20%) and isotropic (80-100%) event classes. Transverse sphericity will henceforth be referred to as *sphericity* for the sake of simplicity.

OBSERVABLES

The mean value of the transverse momentum, obtained for a particular multiplicity class can be defined as

$$\langle\langle p_T \rangle\rangle = \left\langle \frac{\sum_{i=1}^{N_{\text{ch}}} p_i}{N_{\text{ch}}} \right\rangle \quad (2)$$

where N_{ch} denotes the number of charged particles in a single event and p_i represents the transverse momentum of the i^{th} particle in the event. The first average is determined over all of the p_i in an

event, while the second average is carried out over all of the events included in a certain multiplicity class. From this point on, the mean transverse momentum of the particles will be denoted by $\langle\langle p_T \rangle\rangle$.

The two-particle transverse momentum correlator, $\langle\Delta p_i \Delta p_j\rangle$, is constructed as –

$$\langle\Delta p_i \Delta p_j\rangle = \left\langle \frac{\sum_{i,j \neq i} (p_i - \langle\langle p_T \rangle\rangle)(p_j - \langle\langle p_T \rangle\rangle)}{N_{\text{ch}}(N_{\text{ch}} - 1)} \right\rangle \quad (3)$$

Similarly, the three-particle and four-particle correlators are given by

$$\langle\Delta p_i \Delta p_j \Delta p_k\rangle = \left\langle \frac{\sum_{i,j \neq i, k \neq i, j} (p_i - \langle\langle p_T \rangle\rangle)(p_j - \langle\langle p_T \rangle\rangle)(p_k - \langle\langle p_T \rangle\rangle)}{N_{\text{ch}}(N_{\text{ch}} - 1)(N_{\text{ch}} - 2)} \right\rangle \quad (4)$$

$$\langle\Delta p_i \Delta p_j \Delta p_k \Delta p_l\rangle = \left\langle \frac{\sum_{i,j \neq i, k \neq i, j, l \neq i, j, k} (p_i - \langle\langle p_T \rangle\rangle)(p_j - \langle\langle p_T \rangle\rangle)(p_k - \langle\langle p_T \rangle\rangle)(p_l - \langle\langle p_T \rangle\rangle)}{N_{\text{ch}}(N_{\text{ch}} - 1)(N_{\text{ch}} - 2)(N_{\text{ch}} - 3)} \right\rangle \quad (5)$$

These correlators can be written in a more simpler form when expressed in terms of raw moments as follows [23] :

$$\begin{aligned} \langle\langle p_T \rangle\rangle &= \left\langle \frac{Q_1}{N_{\text{ch}}} \right\rangle, \\ \langle\Delta p_i \Delta p_j\rangle &= \left\langle \frac{Q_1^2 - Q_2}{N_{\text{ch}}(N_{\text{ch}} - 1)} \right\rangle - \left\langle \frac{Q_1}{N_{\text{ch}}} \right\rangle^2, \\ \langle\Delta p_i \Delta p_j \Delta p_k\rangle &= \left\langle \frac{Q_1^3 - 3Q_2Q_1 + 2Q_3}{N_{\text{ch}}(N_{\text{ch}} - 1)(N_{\text{ch}} - 2)} \right\rangle - 3 \left\langle \frac{Q_1^2 - Q_2}{N_{\text{ch}}(N_{\text{ch}} - 1)} \right\rangle \left\langle \frac{Q_1}{N_{\text{ch}}} \right\rangle + 2 \left\langle \frac{Q_1}{N_{\text{ch}}} \right\rangle^3. \end{aligned}$$

$$\begin{aligned} \langle\Delta p_i \Delta p_j \Delta p_k \Delta p_l\rangle &= \left\langle \frac{Q_1^4 - 6Q_4 + 8Q_1Q_3 - 6Q_1^2Q_2 + 3Q_2^2}{N_{\text{ch}}(N_{\text{ch}} - 1)(N_{\text{ch}} - 2)(N_{\text{ch}} - 3)} \right\rangle - 4 \left\langle \frac{Q_1^3 - 3Q_2Q_1 + 2Q_3}{N_{\text{ch}}(N_{\text{ch}} - 1)(N_{\text{ch}} - 2)} \right\rangle \left\langle \frac{Q_1}{N_{\text{ch}}} \right\rangle \\ &\quad + 6 \left\langle \frac{Q_1^2 - Q_2}{N_{\text{ch}}(N_{\text{ch}} - 1)} \right\rangle \left\langle \frac{Q_1}{N_{\text{ch}}} \right\rangle^2 - 3 \left\langle \frac{Q_1}{N_{\text{ch}}} \right\rangle^3. \end{aligned}$$

where, Q_n s are the moments of the transverse momentum distributions in an event and is written as

$$Q_n = \sum_{i=1}^{N_{\text{ch}}} (p_i)^n, \quad (6)$$

p_i denotes the transverse momentum of the particle i , and the sum runs over all the charged particles in an event. The different value of n corresponds to different order of the moment.

In order to make the analysis less sensitive to the range in p_i , we normalise the parameters with $\langle\langle p_T \rangle\rangle$. Thus, the final expressions for two-particle and four-particle correlator under the study takes

the following forms –

$$\langle\Delta p_i \Delta p_j\rangle_{\text{final}} = \frac{\sqrt{\langle\Delta p_i \Delta p_j\rangle}}{\langle\langle p_T \rangle\rangle} \quad (7)$$

$$\langle\Delta p_i \Delta p_j \Delta p_k \Delta p_l\rangle_{\text{final}} = \frac{(\langle\Delta p_i \Delta p_j \Delta p_k \Delta p_l\rangle)^{1/4}}{\langle\langle p_T \rangle\rangle} \quad (8)$$

Likewise, in order to make the three-particle cor-

relator dimensionless, it is normalised as follows

$$\gamma_{p_T} = \frac{\langle \Delta p_i \Delta p_j \Delta p_k \rangle}{\langle \Delta p_i \Delta p_j \rangle^{3/2}} \quad (9)$$

Now the obtained version of the three-particle correlator is called standardized skewness, and further has a system size or centrality dependence, which is measured by the number of participant nucleons in the collision process. So, in an effort to eliminate the trivial size dependence, a second measure of the skewness can be obtained.

$$\Gamma_{p_T} = \frac{\langle \Delta p_i \Delta p_j \Delta p_k \rangle \langle p_T \rangle}{\langle \Delta p_i \Delta p_j \rangle^2} \quad (10)$$

Γ_{p_T} is called intensive skewness and is independent of the number of participant nucleons or centrality.

III. RESULTS AND DISCUSSION

The present analysis has been carried out with 100 million events, generated for p–p collisions at $\sqrt{s} = 7$ TeV and 13 TeV using PYTHIA 8 event generator with the standard Monash 2013 tune. The charged particles were accepted in a pseudo-rapidity window of $|\eta| < 0.8$. Further, charged particles having transverse momentum range $0.15 < p_T < 2.0$ GeV/c were considered for this investigation. The event multiplicity estimation was done by classifying the events based on the charged particle multiplicity obtained in the forward (backward) pseudo-rapidity ranges : $2.8 < \eta < 5.1$ and $-3.7 < \eta < -1.7$. The obtained multiplicity values scale linearly with the charged particle multiplicity in the accepted range ($|\eta| < 0.8$), used for the analysis. For each event class, the corresponding mean charged multiplicity, $\langle N_{ch} \rangle$ was obtained in $|\eta| < 0.8$. This was done to avoid auto-correlation biases.

Figure 2 shows the variation of $\langle\langle p_T \rangle\rangle$ as a function of mean charged particle multiplicity $\langle N_{ch} \rangle$ within $|\eta| < 0.8$ for p–p collisions at $\sqrt{s} = 7$ TeV and 13 TeV. The effect of different modes of color reconnections has been shown in the middle panel of Figure 2 for 13 TeV beam energy.

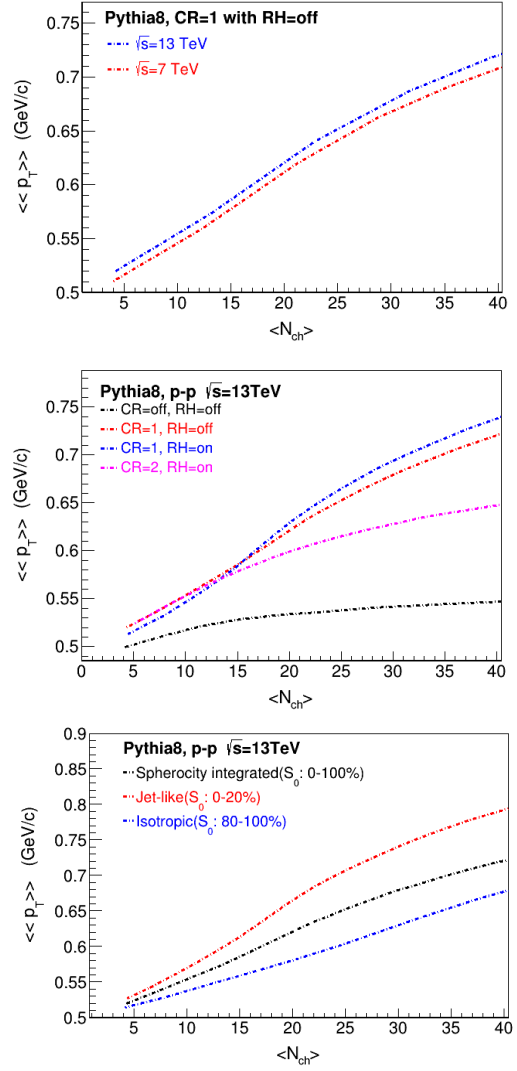


FIG. 2: The top panel shows the variation of $\langle\langle p_T \rangle\rangle$ with $\langle N_{ch} \rangle$ for p–p collisions at $\sqrt{s} = 7$ TeV and 13 TeV. The effect of different modes of color reconnection (CR) on the variation of $\langle\langle p_T \rangle\rangle$ with multiplicity for collision energy $\sqrt{s} = 13$ TeV is shown in the middle panel. The bottom panel shows the variation of $\langle\langle p_T \rangle\rangle$ with $\langle N_{ch} \rangle$ for p–p collisions at $\sqrt{s} = 13$ TeV for different sphericity classes.

One can observe that the $\langle\langle p_T \rangle\rangle$ values are systematically higher for higher collision energy. It can also be observed that switching on the color reconnection (CR) modes increases the $\langle\langle p_T \rangle\rangle$ value of the charged particles. The implementation of CR models in PYTHIA 8 was found to mimic several collective-like behaviour seen in heavy-ion collisions and thus, one is prompted to study the effects

of different CR models on the fluctuation observables. The mean transverse momentum, $\langle\langle p_T \rangle\rangle$ of the charged particles shows a clear rise with the average charged particle multiplicity ($\langle N_{ch} \rangle$), for all CR modes, compared to the case when colour reconnection is turned off (middle panel). The QCD-based CR model (CR=1) with the rope formation exhibits the strongest upward trend. It should be mentioned that the mechanism of color reconnection was originally introduced to explain the increase of $\langle\langle p_T \rangle\rangle$ with charged particle multiplicity. It allows the partonic interactions through color strings from different semi-hard scatterings. There is a prior fusion of strings from different multipartonic systems before hadronization, which leads to a decrease in overall multiplicity but the particles are more energetic and consequently have a higher value of $\langle\langle p_T \rangle\rangle$.

The bottom plot in the Figure 2 shows the variation of $\langle\langle p_T \rangle\rangle$ as a function of average charged particle multiplicity for different sphericity classes. One can observe that the values are significantly higher for the events representing the lower 0-20% sphericity class (Jetty). These are the events dominated by hard scatterings and give rise to di-jet topology. The values for isotropic events (80-100% sphericity class) are consistently lower than those for sphericity integrated (0-100% sphericity) event class. The behaviour is qualitatively similar to the one measured by ALICE experiment [10]. This can be attributed to the dominance of hard scattering events in the lower 0-20% sphericity class, while the 80-100% are dominated by underlying events.

As mentioned earlier, the event-by-event mean transverse momentum fluctuations can be quantified using two-, three- and four- particle correlators. These fluctuations mainly arises from the initial state fluctuations and contain relevant information about the underlying physical processes of particle production [23].

Figure 3 depicts the fluctuation of the two-particle correlator for p-p collisions at $\sqrt{s} = 7$ and 13 TeV as a function of charged particle multiplicity. It can be observed that the strength of the

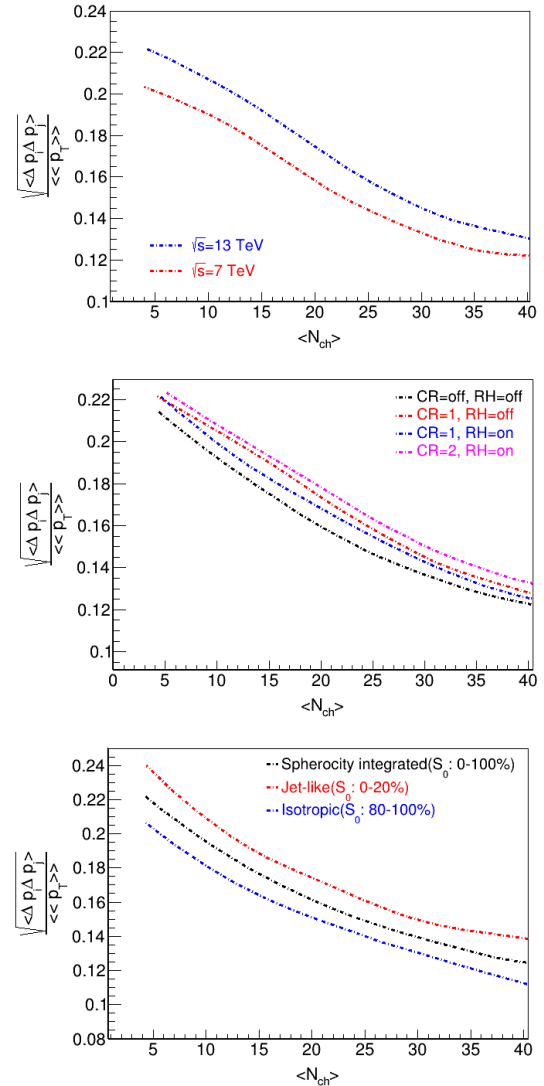


FIG. 3: The variation of two-particle correlator at $\sqrt{s} = 7$ and 13 TeV as a function of $\langle N_{ch} \rangle$. The middle panel shows the effect of different color reconnection models at $\sqrt{s} = 13$ TeV. The bottom panel shows the variation of two-particle correlator with $\langle N_{ch} \rangle$ in different sphericity classes.

two-particle correlator decreases with an increase of the average multiplicity. This can be attributed to the independent superposition of multi-partonic interactions in p-p collisions. However, the values at $\sqrt{s} = 13$ TeV are systematically higher than that observed at 7 TeV, indicating an energy dependence of the observable. The middle panel of the Figure 3 shows the effect of various modes of color reconnections on the strength of the corre-

lator. The mechanism of color reconnection increases the correlation strength due to enhanced partonic interactions via color strings. The interplay of rope formation in different CR modes also causes a difference in the strength of the correlator. The variation of the two-particle correlator as a function of multiplicity was also compared for three different sphericity classes as shown in Figure 3. One can observe that the values are higher for the lower 0-20% sphericity class (Jetty), indicating that significant contribution comes from the di-jets in low sphericity classes.

Recently, it was shown in the reference [23] that event-by-event fluctuations of the $\langle\langle p_T \rangle\rangle$ in heavy-ion collisions exhibit a positive skew, as predicted by hydrodynamic evolution of the medium. The idea stemmed from the strong correlation of transverse momentum fluctuations with the fluctuations of the initial energy of the fluid. An estimation of the three-particle correlation using standardized and intensive skewness for p–p collisions at $\sqrt{s} = 7$ and 13 TeV is shown in the Figure 4 and 5, respectively. Assuming that the dynamical and statistical fluctuations scale inversely with multiplicity [23], the standardized skewness is expected to be larger for lower multiplicity classes. It is indeed observed that γ_{p_T} exhibits a sharp diminishing trend upto a charged particle multiplicity range of 15 and saturates thereafter. However, the magnitude is considerably higher when compared to hydrodynamic predictions for heavy-ion collisions. This trend is also seen for intensive skewness, Γ_{p_T} which was introduced to eliminate the volume dependence in heavy-ion collisions. Although, p–p system is not affected by volume fluctuations, studying the variation of Γ_{p_T} is interesting to form a baseline. Like γ_{p_T} , the values of Γ_{p_T} are higher for low multiplicity events and gradually saturates after 15. In addition, the comparisons of various CR models (middle panels of Fig. 4, 5) revealed a decrease in the correlation strength when CR was introduced. This could indicate that the color string fusion dominantly affects (or enhances) the two-particle correlation and does not have any significant effect on higher order correlations. The sphericity comparisons of the three-particle correlator

indicates higher correlation for jetty events (0-20% sphericity class), whilst the isotropic events (80-100% sphericity class) have lower values. (Fig. 4 and 5).

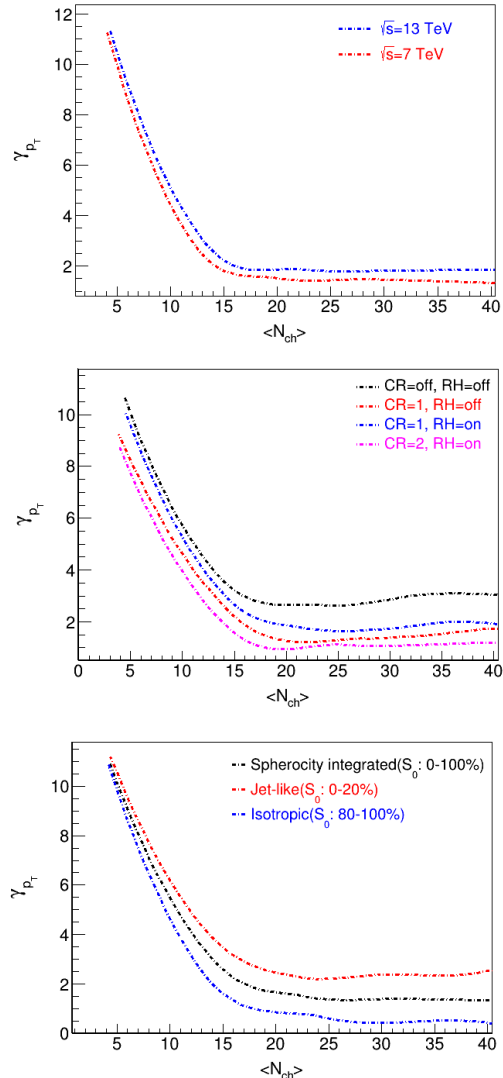


FIG. 4: The energy dependence (top) and the effect of different color reconnection (CR) model comparison (middle) of γ_{p_T} in p–p collisions at $\sqrt{s} = 7$ TeV and 13 TeV. The bottom panel shows its variation in different sphericity classes at $\sqrt{s} = 13$ TeV.

The study was further extended to observe the variation of the four-particle correlator with mean charged particle multiplicity for p–p collisions at $\sqrt{s} = 7$ and 13 TeV as shown in Figure 6. These types of studies are subjected to large statistics and can reveal crucial information on the higher order

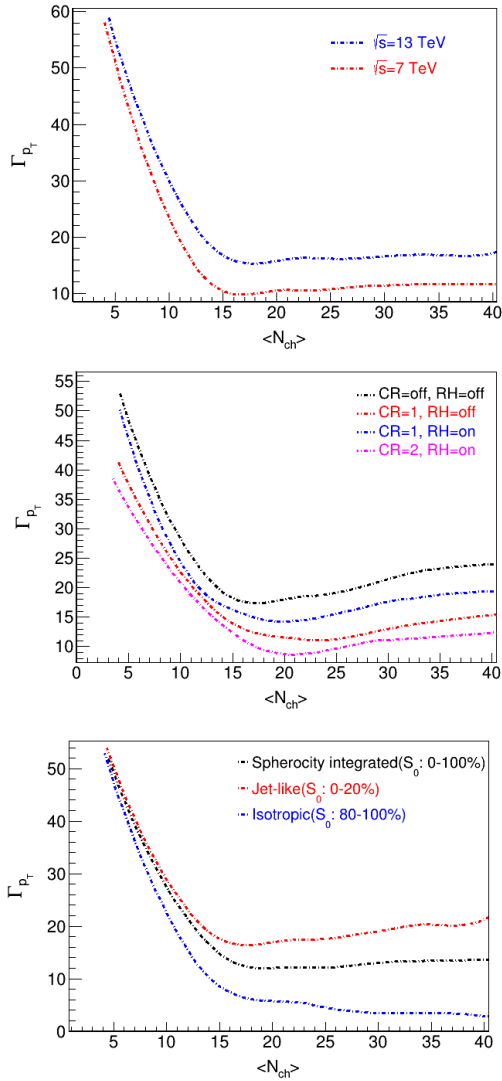


FIG. 5: The energy dependence (top) and the effect of different color reconnection (CR) model comparison (middle) of Γ_{p_T} in p - p collisions at $\sqrt{s} = 7$ TeV and 13 TeV. The bottom panel shows its variation in different sphericity classes at $\sqrt{s} = 13$ TeV.

correlation strength. It is observed that the correlator shows a smooth decreasing trend towards higher multiplicity classes. The increase in parton activity that causes the parton's terminal strings to recombine— known as color reconnection, produces a weaker trend in the correlation function. This trend is weakest in case of a color reconnection model CR=2 which is based on the movement of gluons in order to produce a string of minimum tension. Further, sphericity investigation shows

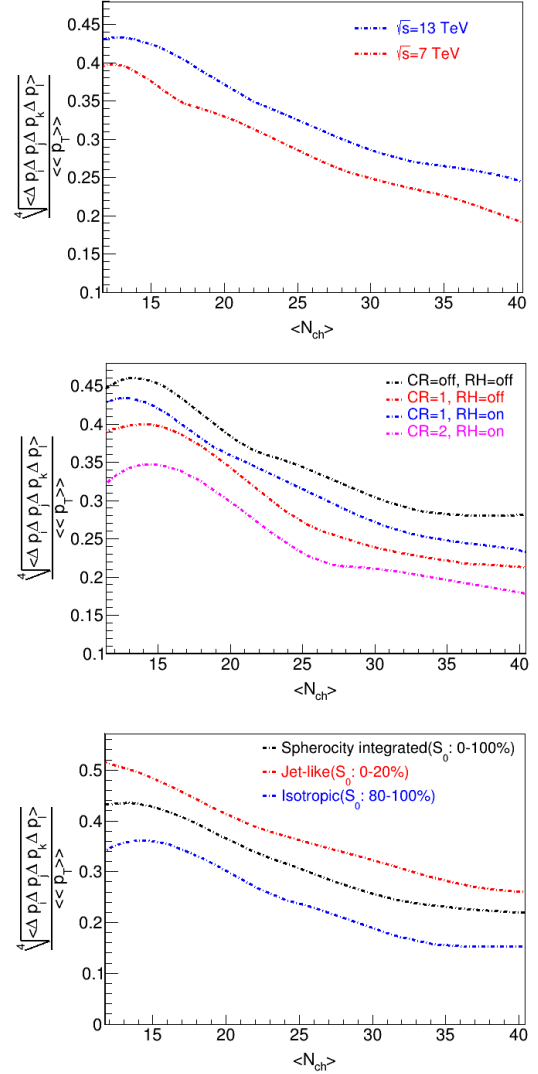


FIG. 6: The four-particle correlator as a function of $\langle N_{ch} \rangle$ for different energies (top) and color reconnection (CR) models (middle). The bottom panel shows the correlator strength in different sphericity classes at $\sqrt{s} = 13$ TeV.

that the correlations are strongest for events dominated by hard scattering (lower 0-20% sphericity class).

IV. SUMMARY

Event-by-event fluctuation of the mean transverse momentum ($\langle p_T \rangle$) has been studied as a function of average charged particle multiplicity

$\langle\langle N_{\text{ch}} \rangle\rangle$ in p–p collisions at $\sqrt{s} = 7$ TeV and 13 TeV using the PYTHIA 8 event generator. The charged particles were selected from a kinematic range of $0.15 < p_{\text{T}} < 2$ GeV/ c and $|\eta| < 0.8$. The dynamical fluctuations of the mean transverse momentum is caused by fluctuation in the early stages of the collision systems and have been measured using two-, three-, and four-particle correlators. A characteristic decrease of the two-particle particle correlator with the charged particle multiplicity is observed. This phenomenon is attributed to independent superposition of multi-partonic interaction in p–p collisions. The effects of various microscopic processes like color reconnection and multi-partonic interactions has also been investigated. The mechanism of color reconnections with rope formation scenario showed higher correlation. Higher order (third and fourth) correlation functions, which have been reported for the

first time, did not, however, exhibit the same behaviour. The study also suggests an energy dependence of the mean transverse momentum fluctuation in p–p collisions at $\sqrt{s} = 7$ TeV and 13 TeV. Furthermore, the fluctuation observable has also been studied in different intervals of transverse sphericity to understand the relative contributions originating from hard scattering and underlying events. It was observed that the correlations were always stronger for events with di-jet-like topology. The present study in p–p collisions would act as a baseline for the upcoming measurements in A–A as well as p–p collisions at the LHC.

V. ACKNOWLEDGEMENTS

The authors would like to thank the Department of Science and Technology (DST), India for supporting the present work.

-
- [1] J. Adams et al, STAR Collaboration, Phys. Rev. **C 72**, 044902 (2005).
 - [2] B. B. Abelev et al, ALICE Collaboration, Eur. Phys. J. **C 74**, 3077 (2014).
 - [3] T. A. Trainor, Phys. Rev. **C 92**, 024915 (2015).
 - [4] L. Stodolsky, Phys. Rev. Lett. **75**, 1044 (1995).
 - [5] J. Adams et al, STAR Collaboration, Phys. Rev. **C 99**, 044918 (2019).
 - [6] S. Voloshin, Phys. Lett. **B 632**, 490-494 (2006).
 - [7] B. Schenke, Chun Shen and Derek Teaney, Phys. Rev. **C 102**, 034905 (2020).
 - [8] P. Bartalini, E. Berger, B. Blok, G. Calucci, R. Corke, et al., arXiv:1111.0469 [hep-ph]
 - [9] Torbjörn Sjöstrand, Stefan Ask, Jesper R Christiansen, Richard Corke, Nishita Desai, Philip Ilten, Stephen Mrenna, Stefan Prestel, Christine O Rasmussen, and Peter Z Skands, Comput. phys. commun. **191**, 159–177 (2015).
 - [10] B. B. Abelev et al, ALICE Collaboration, Phys. Lett. **B 727**, 371 (2013).
 - [11] Torbjörn Sjöstrand, arXiv:1310.8073,(2013).
 - [12] Christian Bierlich and Jesper Roy Christiansen, Phys. Rev **D 92**,094010 (2015).
 - [13] Jesper Roy Christiansen and P. Z.Skands, JHEP, **08**, 003 (2015).
 - [14] T. S. Biro, H. B. Nielson and J. Knoll, Nucl. Phys. **B 245**, 449, (1984).
 - [15] C.Bierlich, G. Gustafson, L. Lonnblad and A. Tarasov, J. High Energ. Phys. **2015: 148**, (2015).
 - [16] Ranjit Nayak, Subhadip Pal, and Sadhana Dash, Phys. Rev. **D 100**, 074023 (2019).
 - [17] Pritam Chakraborty and Sadhana Dash, Phys. Rev. **C 102**, 055202 (2020).
 - [18] Ankita Goswami, Ranjit Nayak, Basanta Kumar Nandi, and Sadhana Dash, Eur. Phys. J. **C 81**, 988 (2021).
 - [19] T. Pierog, Iu. Karpenko, J. M. Katzy, E. Yatsenko, and K. Werner, Phys. Rev **C 92**, 034906 (2015).
 - [20] A. Banfi, G. P. Salam, and G. Zanderighi, JHEP **06**, 038 (2010).
 - [21] A. Ortiz, G. Paic, and E. Cuautle, Nucl. Phys. **A 941**, 78-86 (2015).
 - [22] S. Acharya et al, ALICE Collaboration, Eur. Phys. J. **C 79**, 857 (2019).
 - [23] Giuliano Giacalone, Fernando G. Gardim, Jacquelyn Noronha-Hostler, and Jean-Yves Ollitrault, Phys. Rev. **C 103**, 024910 (2021).